# Modeling the Bistable Dynamics of the Innate Immune System

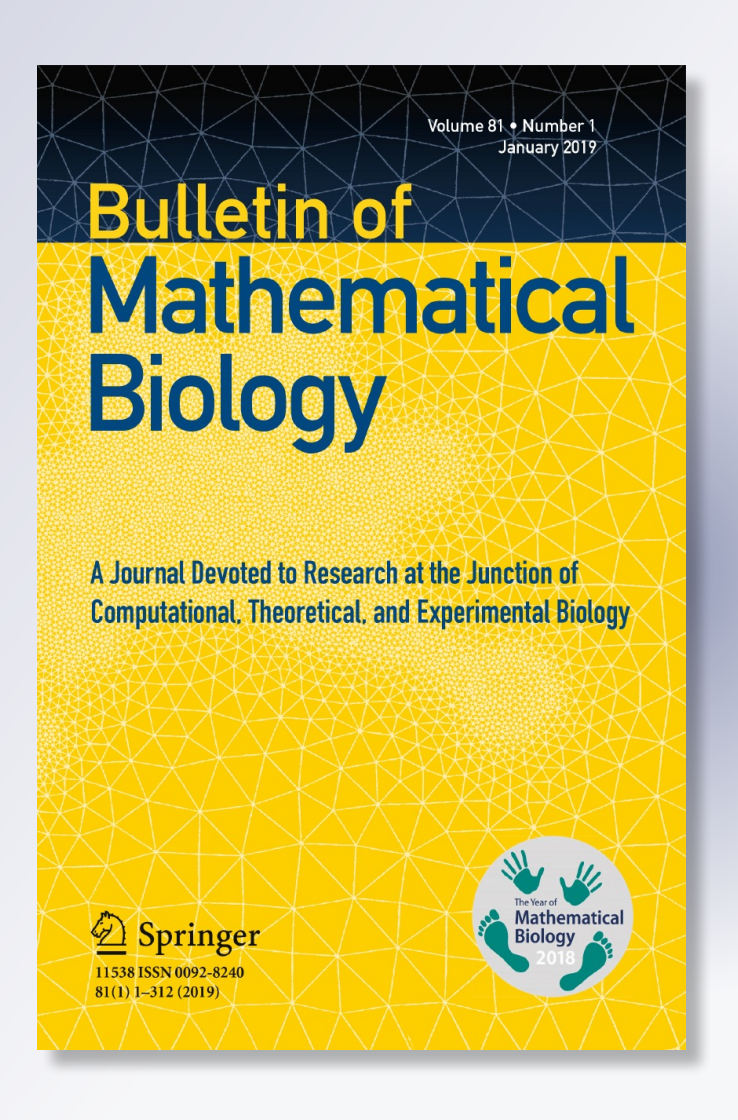
# Sarah Kadelka, Brittany P. Boribong, Liwu Li & Stanca M. Ciupe

## **Bulletin of Mathematical Biology**

A Journal Devoted to Research at the Junction of Computational, Theoretical and Experimental Biology Official Journal of The Society for Mathematical Biology

ISSN 0092-8240 Volume 81 Number 1

Bull Math Biol (2019) 81:256-276 DOI 10.1007/s11538-018-0527-y





Your article is protected by copyright and all rights are held exclusively by Society for Mathematical Biology. This e-offprint is for personal use only and shall not be selfarchived in electronic repositories. If you wish to self-archive your article, please use the accepted manuscript version for posting on your own website. You may further deposit the accepted manuscript version in any repository, provided it is only made publicly available 12 months after official publication or later and provided acknowledgement is given to the original source of publication and a link is inserted to the published article on Springer's website. The link must be accompanied by the following text: "The final publication is available at link.springer.com".



## Author's personal copy

Bulletin of Mathematical Biology (2019) 81:256–276 https://doi.org/10.1007/s11538-018-0527-y





# Modeling the Bistable Dynamics of the Innate Immune System

Sarah Kadelka<sup>1</sup> · Brittany P. Boribong<sup>2</sup> · Liwu Li<sup>3</sup> · Stanca M. Ciupe<sup>1</sup>

Received: 30 November 2017 / Accepted: 22 October 2018 / Published online: 1 November 2018 © Society for Mathematical Biology 2018

#### **Abstract**

The size of primary challenge with lipopolysaccharide induces changes in the innate immune cells phenotype between pro-inflammatory and pro-tolerant states when facing a secondary lipopolysaccharide challenge. To determine the molecular mechanisms governing this differential response, we propose a mathematical model for the interaction between three proteins involved in the immune cell decision making: IRAK-1, PI3K, and RelB. The mutual inhibition of IRAK-1 and PI3K in the model leads to bistable dynamics. By using the levels of RelB as indicative of strength of the immune responses, we connect the size of different primary lipopolysaccharide doses to the differential phenotypical outcomes following a secondary challenge. We further predict under what circumstances the primary LPS dose does not influence the response to a secondary challenge. Our results can be used to guide treatments for patients with either autoimmune disease or compromised immune system.

**Keywords** Innate immunity · Bistable dynamics · Mathematical modeling

#### 1 Introduction

The human innate immune system responds immediately to foreign challenges by sending various signals to immune cells to migrate toward the site of the infection and destroy the offending microbe (Janeway et al. 2001). The innate immune system can initiate an immune response in several ways, including signaling the start of an inflammatory response. Pro-inflammatory cytokines are released, signaling monocytes within the bloodstream to differentiate into macrophages, migrate toward the site

Department of Biological Sciences, Virginia Tech, Blacksburg, VA, USA



Stanca M. Ciupe stanca@math.vt.edu

Department of Mathematics, Virginia Tech, Blacksburg, VA, USA

Interdisciplinary Program in Genetics, Bioinformatics and Computational Biology, Virginia Tech, Blacksburg, VA, USA

of infection, and phagocytose invading microbes. Macrophages in turn will release pro-inflammatory cytokines themselves to recruit more cells, thus upregulating an inflammatory response within the immune system (Shi and Pamer 2011). The innate immune system acts ahead of the adaptive immune system due to its in-born ability to recognize and destroy nonspecific stimuli. It is thought, however, that it does not generate any memory to repeated challenges (Sun et al. 2014). It has been recently shown that, depending on the strength of the primary stimuli, the innate immune system can exhibit either a pro-inflammatory or pro-resolvent response when acted upon by secondary stimuli, suggesting that memory may be a characteristic of innate immunity after all (Morris and Li 2012). Understanding the mechanistic interactions leading to the differential responses between the two phenotypes and predicting how a state can be avoided can guide treatment development for diseases in which the patient is experiencing either immunodeficiency or an overactive immune response.

A switch between inflammation and tolerance has been observed in the response of macrophages to lipopolysaccharide (LPS), a strong inflammatory stimulant derived from gram-negative bacteria (Chen et al. 2009; Morris and Li 2012). Different primary doses of LPS will prompt specialized macrophage functions (Dillingh et al. 2014). High primary LPS doses (10–100 ng/ml) trigger inflammation in the form of high-level cytokine production with sometimes fatal consequences (Hirohashi and Morrison 1996; Shnyra et al. 1998; Hume et al. 2001). Such responses can be reprogrammed by administration of more than one LPS challenge. In particular, a primary challenge with super-low-dose LPS (0.05–1 ng/ml) followed by a subsequent boosting with high-dose LPS (10–100 ng/ml) leads to macrophage priming (Hirohashi and Morrison 1996; Shnyra et al. 1998; West and Koons 2008; Zhang and Morrison 1993). Macrophages become fully activated through signaling pathways, and start producing pro-inflammatory cytokines (Deng et al. 2013; Zhang and An 2007) such as IRAK-1 and PI3K. In addition to greater production of pro-inflammatory cytokines, macrophage priming also blocks the production of anti-inflammatory cytokines such as RAR $\alpha$  and ROR $\alpha$ , allowing for a non-resolving inflammation within the system (Maitra et al. 2011; Yuan and Li 2016). By contrast, a primary challenge with highdose LPS (10–100 ng/ml) followed by a subsequent boosting with high-dose LPS (10–100 ng/ml) leads to suppression of pro-inflammatory signals, or an LPS-induced tolerance (Biswas and Lopez-Collazo 2009; West and Heagy 2002). Tolerance is characterized by the suppression of pro-inflammatory cytokines, such as IL-12 and TNF- $\alpha$ (Wysocka et al. 2001; Ma et al. 2015; Medvedev et al. 2000; Ziegler-Heitbrock 1995), which results in an acute, transient inflammatory response.

One transcription factor influencing an innate immune cell's phenotype is RelB, which blocks transcription of pro-inflammatory mediators by assembling a suppressive complex on their promoters (Chen et al. 2009; Deng et al. 2013). Differences in the primary LPS dose alter the upstream molecular mechanisms that regulate the production of RelB, such as the dynamics of the kinases phosphoinositide 3-kinase (PI3K), and interleukin receptor-associated kinase 1 (IRAK-1). In particular, LPS lowers IRAK-1 production and increases PI3K activation. In return, PI3K enhances RelB and inhibits IRAK-1 productions, while IRAK-1 degrades RelB (Deng et al. 2013). Therefore, super-low primary LPS dose results in low RelB production and high primary LPS dose results in high RelB production. The interactions between



these three proteins contribute to the emergence of primed and tolerant macrophage responses, although due to the complex nature of the intracellular signaling networks, it is difficult to present a quantitative understanding of how a state is achieved based on the size of LPS.

To shed light on the molecular mechanisms governing the differential responses between tolerance and immune exacerbation and into their connection to the LPS levels, we investigate the molecular network describing the phenotypical response, i.e., the interactions between RelB, IRAK-1 and PI3K. Previous models looking at priming and tolerance due to endotoxin challenge were abstract and did not look at specific protein interactions (Day et al. 2006; Reynolds et al. 2006), which makes our model novel and informative. In particular, we are interested in understanding the types and levels of feedbacks between the three nodes of the network. Since experimental testing of the roles of each molecule is expensive and time-consuming, we use mathematical models to predict the motifs behind the differential response. Such models are inexpensive and easy to manipulate, and their predictions can help guide experiments. Our focus lies on explaining a possible mechanism yielding different RelB levels depending on the strength of LPS. We develop a deterministic mathematical model with bistable dynamics yielding different RelB levels at equilibrium based on the initial levels of IRAK-1, PI3K, RelB, and LPS. The model has bistable dynamics. We use the variables kinetics and their role in macrophage behavior to connect the size of secondary LPS doses with the rise of pro-inflammatory or pro-tolerant macrophage phenotypes. Quantifying lipopolysaccharide doses leading to macrophage priming may offer significant advantage in inducing an adaptive-like defense against invading pathogens. Similarly, quantifying lipopolysaccharide doses leading to macrophage tolerance may help control the induction of immunosuppression.

### 2 Mathematical Modeling of Priming and Tolerance

#### 2.1 Model

We consider the interactions between three proteins IRAK-1 (x), PI3K (y), and ReIB (z) in the presence of LPS (L). It has been reported that LPS induces IRAK-1 and PI3K production (Chaurasia et al. 2010; Huang et al. 2004; Guha and Mackman 2001). For simplicity, and in the absence of other information, we assume that the LPS effect on IRAK-1 and PI3K production is linear. Hence, IRAK-1 and PI3K are produced at rates  $c_x + a_x L$  and  $c_y + a_y L$ , respectively. IRAK-1 and PI3K are competing intracellular players (Deng et al. 2013; Fan and Cook 2004; Noubir et al. 2004; Chaurasia et al. 2010). We reflect this competition by modeling a mutual inhibition between these two proteins, with IRAK-1 being inhibited by PI3K at rate  $1/(b_x^m + y^m)$  and PI3K being inhibited by IRAK-1 at rate  $1/(b_y + x)$ , where  $b_x$  and  $b_y$  are the y and x values where the inhibition is half maximal. By modeling this mutual inhibition, we account for the experimentally observed opposing modulations of LPS on IRAK-1 and PI3K (Deng et al. 2013). We further assume that IRAK-1 decays at per capita rate  $d_x$  and that PI3K is lost (in a density-dependent manner) at rate  $d_y/(b_v + y)$ , where  $d_y$  is the maximal loss rate and  $b_v$  is the y where the loss is half maximal (Goldbeter 1995). It



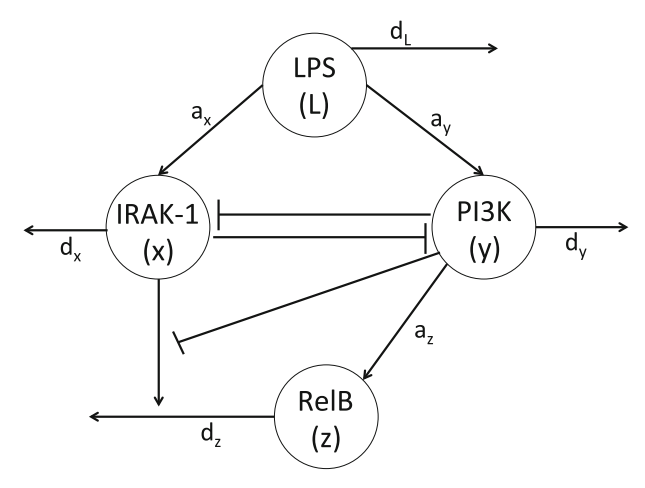


Fig. 1 Model schematic

has been shown (Deng et al. 2013) that RelB production is enhanced by PI3K, while its loss is enhanced by IRAK-1 and inhibited by PI3K. We model this by assuming an PI3K-induced production at rate  $a_z y/(b_z + y)$ , where  $a_z$  is the maximal production rate and  $b_z$  is the y where the production is half maximal. Moreover, we model the degradation term to be  $d_z z x/(b_z + y)$ , where  $d_z$  is the maximal degradation rate and  $b_z$  is the y where the loss is half maximal. Lastly, following initial inoculation, LPS decays exponentially at per capita rate  $d_L$ . A schematic diagram of these interactions is shown in Fig. 1, and the mathematical representation is given by the following system

$$\frac{\mathrm{d}x}{\mathrm{d}t} = \frac{c_x + a_x L}{b_x^m + y^m} - d_x x,$$

$$\frac{\mathrm{d}y}{\mathrm{d}t} = \frac{c_y + a_y L}{b_y + x} - d_y \frac{y}{b_v + y},$$

$$\frac{\mathrm{d}z}{\mathrm{d}t} = \frac{a_z y}{b_z + y} - d_z z \frac{x}{b_z + y},$$

$$\frac{\mathrm{d}L}{\mathrm{d}t} = -d_L L,$$
(1)

where  $c_x = c_y = 0$  if L = 0 and  $c_x$ ,  $c_y \neq 0$  if  $L \neq 0$ .

For simplicity, we assume that the inhibition rates  $b_x^m = b_y = b_z = b_v = 1$ . In an unstimulated cell that never encountered LPS, the proteins IRAK-1, PI3K or RelB are not activated and at an equilibrium value (Arango Duque and Descoteaux 2014). Therefore, in the absence of LPS, variables x, y and z are assumed to be zero. Since model (1) is created to consider previously unstimulated cells, we choose this equilibrium state as our initial condition, i.e.,  $x(0) = x_0 = 0$ ,  $y(0) = y_0 = 0$ ,  $z(0) = z_0 = 0$ . Further,  $z(0) = z_0 = 0$  is the stimulus size of the LPS challenge. One can show that for  $z_y < d_y$ , all solutions of system (1) with positive initial conditions are positive and bounded. Therefore, this model is biologically feasible (see "Appendix").



#### 2.2 Parameter Acquisition

We assume that, in the absence of the LPS stimulus, there are no interactions between IRAK-1, PI3K, and RelB. Thus, the model becomes

$$\frac{\mathrm{d}x}{\mathrm{d}t} = -d_x x, 
\frac{\mathrm{d}y}{\mathrm{d}t} = -d_y \frac{y}{1+y}, 
\frac{\mathrm{d}z}{\mathrm{d}t} = -d_z z.$$
(2)

Moreover, based on experimental findings, we know that (in the absence of LPS) the IRAK-1, PI3K, and RelB's half-lives are 5 h, 0.25 h and 2.5 h (Yamin and Miller 1997; Kollewe et al. 2004; Ko et al. 2014; Abd-Ellah et al. 2018). Solutions of (2) with initial  $y(0) = y_0 = 0$  yield degradation parameters (see Table 1)

$$d_x = \frac{\ln(2)}{5 \,\text{h}} = 0.138 \,\text{h}^{-1},$$

$$d_y = \frac{\frac{1}{2}y_0 + \ln(2)}{0.25 \,\text{h}} = 2.773 \,\text{h}^{-1},$$

$$d_z = \frac{\ln(2)}{2.5 \,\text{h}} = 0.277 \,\text{h}^{-1}.$$
(3)

The half-lives of the three proteins change when acted upon by an endotoxin challenge, with the change being dependent on the size of the stimulus. We assume that when LPS stimulus is present, proteins IRAK-1, PI3K and RelB interact according to model (1), and connect their measured half-lives with the sizes of their equilibria. That is, a low (or zero) equilibrium is representative of fast decay and short half-lives. Conversely, high equilibria corresponds to slow decay and large half-lives.

In the next section, we analytically investigate the equilibria of system (1).

#### 2.3 Stability Analysis

Let  $E = (\bar{x}, \bar{y}, \bar{z}, \bar{L})$  be the IRAK-1, PI3K, RelB, and LPS equilibria. Further let  $A = \frac{c_y}{d_x}$  and  $B = \frac{c_x}{d_x}$ . Then

$$\begin{split} \bar{L} &= 0, \\ \bar{x} &= \frac{B}{1 + \bar{y}^m}, \\ \bar{z} &= \frac{a_z}{d_z} \cdot \frac{\bar{y}}{\bar{x}}, \end{split} \tag{4}$$

where  $\bar{y}$  satisfies the equation

$$\frac{B}{1 + \bar{v}^m} - \frac{A(1 + \bar{y}) - \bar{y}}{\bar{v}} = 0.$$



261

Parameter	Description	Value	Unit	Reference
$d_X$	Decay of IRAK-1	0.138	$h^{-1}$	Yamin and Miller (1997) and Kollewe et al. (2004)
$d_y$	Decay of PI3K	2.773	$h^{-1}$	Ko et al. (2014)
$d_{z}$	Decay of RelB	0.277	$h^{-1}$	Abd-Ellah et al. (2018)
$c_{x}$	Production of IRAK-1	3		
$a_{\chi}$	Production of IRAK-1	1		
$c_y$	Production of PI3K	2.5		
$a_y$	Production of PI3K	1		
$a_z$	Production of RelB	1		
$d_L$	Decay of LPS	0.1	$h^{-1}$	
m		5		

Table 1 Parameter values

We search the parameter space allowing for one or three biologically realistic equilibria and investigate their stability. In order to ensure biological relevance of our model, we only consider parameter sets for which  $c_y < d_y$ . When two locally asymptotically stable equilibria arise, we talk about bistability. For bistability to occur, we have to find at least three equilibria, since two locally asymptotically stable equilibria are always separated by an unstable one. As shown in the "Appendix", a necessary, but not sufficient condition for equations (4) to have three positive solutions is given by

$$m > 1. (5)$$

An equilibrium solution is locally asymptotically stable if it satisfies the condition

$$\frac{AB}{m} > \bar{y}^{m+1}\bar{x}^2,\tag{6}$$

and unstable otherwise (see "Appendix"). If condition (5) is satisfied, then there is either exactly one equilibrium that is locally asymptotically stable or there are two locally asymptotically stable and one unstable equilibrium (see "Appendix"). This shows that our results are robust to parameter choices. Since analytical investigation is challenging, we choose a set of unitless parameter values that satisfy (5) (see Table 1) and use them to numerically find the equilibria (4) and their stability (6).

For the parameters given in Table 1, the equilibria (4) of system (1) are

$$E_1 = (3.39 \times 10^{-4}, 9.14, 9.72 \times 10^4, 0),$$
 (7)

$$E_2 = (21.64, 4.15 \times 10^{-2}, 6.91 \times 10^{-3}, 0),$$
 (8)

$$E_3 = (0.28, 2.38, 30.54, 0).$$
 (9)



The references for the decay rates give half-lives, which we converted to decay rates as described above

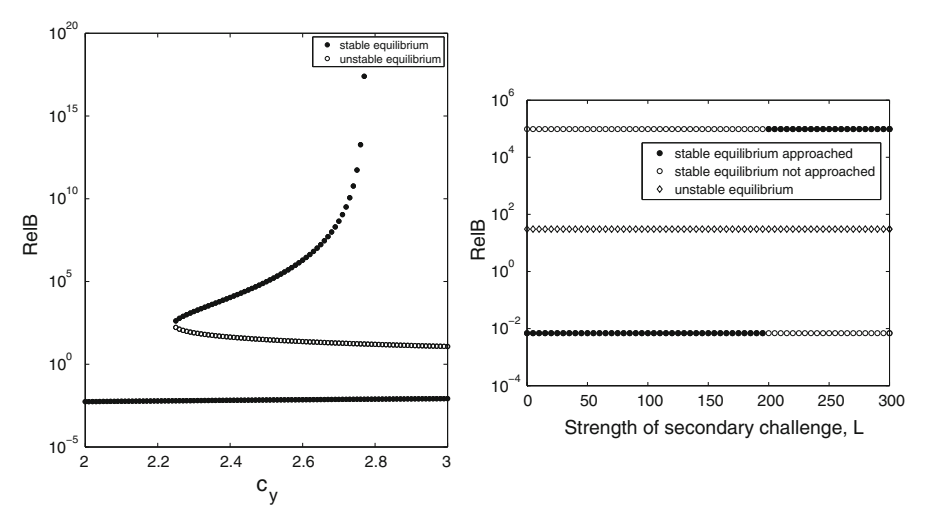


Fig. 2 Left: bifurcation—RelB equilibria versus parameter  $c_y$ . All other parameters as in Table 1; right: dependence of the asymptotically approached RelB equilibrium following secondary challenge 150 h past primary low challenge on the strength of the secondary challenge, when  $c_y = 2.5$ 

Using the stability condition (6), we can show that  $E_1$  and  $E_2$  are locally asymptotically stable and  $E_3$  is unstable. The two locally asymptotically stable equilibria correspond to low RelB  $\approx 0$  ( $E_2$ ) and high RelB  $\approx 97156$  ( $E_1$ ). Since RelB levels are indicative of the pro-inflammatory and pro-resolution phenotypes, we are interested in determining when each equilibrium is reached. It is known that the long-term behavior of bistable systems is determined by the choice of initial conditions. For system (1), long-term dynamics are determined by the initial conditions of IRAK-1, PI3K, and LPS, and are unaffected by the initial RelB. Furthermore, since

$$\bar{z} = \frac{a_z}{d_z} \cdot \frac{\bar{y}}{\bar{x}},\tag{10}$$

the equilibrium size of RelB depends on the size of ratio of PI3K to IRAK-1 equilibria, rather than their individual equilibrium values.

For different choices of parameter values, the bistability may be lost. Fixing all parameters as in Table 1 and varying  $c_y$  yields the hysteretic bifurcation diagram shown in the left panel of Fig. 2. We observe that for an IRAK-1 production rate  $c_y$  in [2.25, 22.3], we obtain two stable equilibria, one with high and one with low (close to zero) RelB value, separated by an unstable equilibrium. For  $0 < c_y < 2.25$  and  $c_y > 22.3$ , only one locally asymptotically stable RelB equilibrium exists. The corresponding relationship between the strength of secondary LPS challenge and the equilibrium values of RelB is shown in the right panel of Fig. 2 for fixed  $c_y = 2.5$ . As expected, low and high secondary LPS correspond to low RelB equilibrium levels, while super-high RelB corresponds to high RelB equilibrium levels.

Next, we will numerically investigate the relationship between the size of RelB equilibria and the LPS levels during primary and secondary challenges.



#### 3 Results

#### 3.1 Primary Challenge

We first examine the dynamics of RelB, IRAK-1, and PI3K after a single LPS challenge. We assume that  $L_0 = 100 (L_0 = 0.1)$  correspond to high (super low) endotoxin challenges,  $x_0 = y_0 = z_0 = 0$ , and all parameters are given in Table 1. A super-low LPS challenge leads to IRAK-1's exponential increase to 21.64 (see Fig. 3a, solid curve). Contrarily, a high LPS challenge leads to an initial short spike in IRAK-1 followed by an exponential decrease to  $1.9 \times 10^{-9}$  within the first 150h (see Fig. 3a, dashed curve). We can further connect these outcomes to the qualitative differences in IRAK-1 half-lives for different LPS stimuli observed experimentally. Indeed, our model predicts that for a super-low LPS stimulus IRAK-1 increases following its initial spike due to activation, matching the long half-life of 5 h observed experimentally (Kollewe et al. 2004). In contrast, for high LPS stimulus IRAK-1 decreases, matching the shorter half-life of 0.5 h observed experimentally (Kollewe et al. 2004). For the other two proteins, PI3K and RelB, the model predicts exponential decreases to  $4.1 \times 10^{-2}$  and  $6.9 \times 10^{-3}$ , respectively, for super-low LPS stimuli (see Fig. 3c, e, solid curves). In contrast, the model predicts increases to 549.2 and 149.4, respectively, for high LPS challenge (see Fig. 3c, e, dashed curves). As with IRAK-1, these results match the experimental PI3K and RelB's half-lives: 2.5 and 3h for high LPS challenge (Ko et al. 2014; Abd-Ellah et al. 2018), 0.25 and 0.5 h for super-low LPS challenge (Ko et al. 2014; Abd-Ellah et al. 2018).

We observe that the RelB level is high (low) following super-low (high) primary LPS challenge as seen in experiments (Deng et al. 2013). Since RelB is responsible for blocking the transcription of inflammatory mediators (Deng et al. 2013), an initial low RelB level can trigger a strong inflammatory response. We next investigate how this initial reaction changes when RelB response is reprogrammed through two consecutive LPS challenges.

#### 3.2 Secondary Challenge Without a Phenotype Switch

We next examine how the strength of the primary LPS challenge influences the system's dynamics following a secondary high LPS encounter. We assume that super-low (high) primary LPS challenge is followed by high LPS booster (with  $L_0 = 100$ )  $\tau = 150\,\mathrm{h}$  later. The initial conditions for the other variables are set at x(150), y(150) and z(150) in the primary challenge model. Figure 3b, d, f shows the emerging dynamics. Our model shows that when we consider two consecutive high LPS challenges, IRAK-1 decreases exponentially to a low equilibrium (Fig. 3b, dashed curve). PI3K and RelB increase from 549.2 to 1508.6, and 149.4 to 305.9, respectively, (Fig. 3d, f, dashed curve). Even though the absolute values of all three proteins change between primary and boosting stimuli, their values during both primary and secondary responses are representative of a weak inflammatory response which we associate with immune tolerance. Similarly, when we model the RelB dynamics during a super-low LPS primary challenge followed by a high LPS booster, the asymptotic dynamics of the



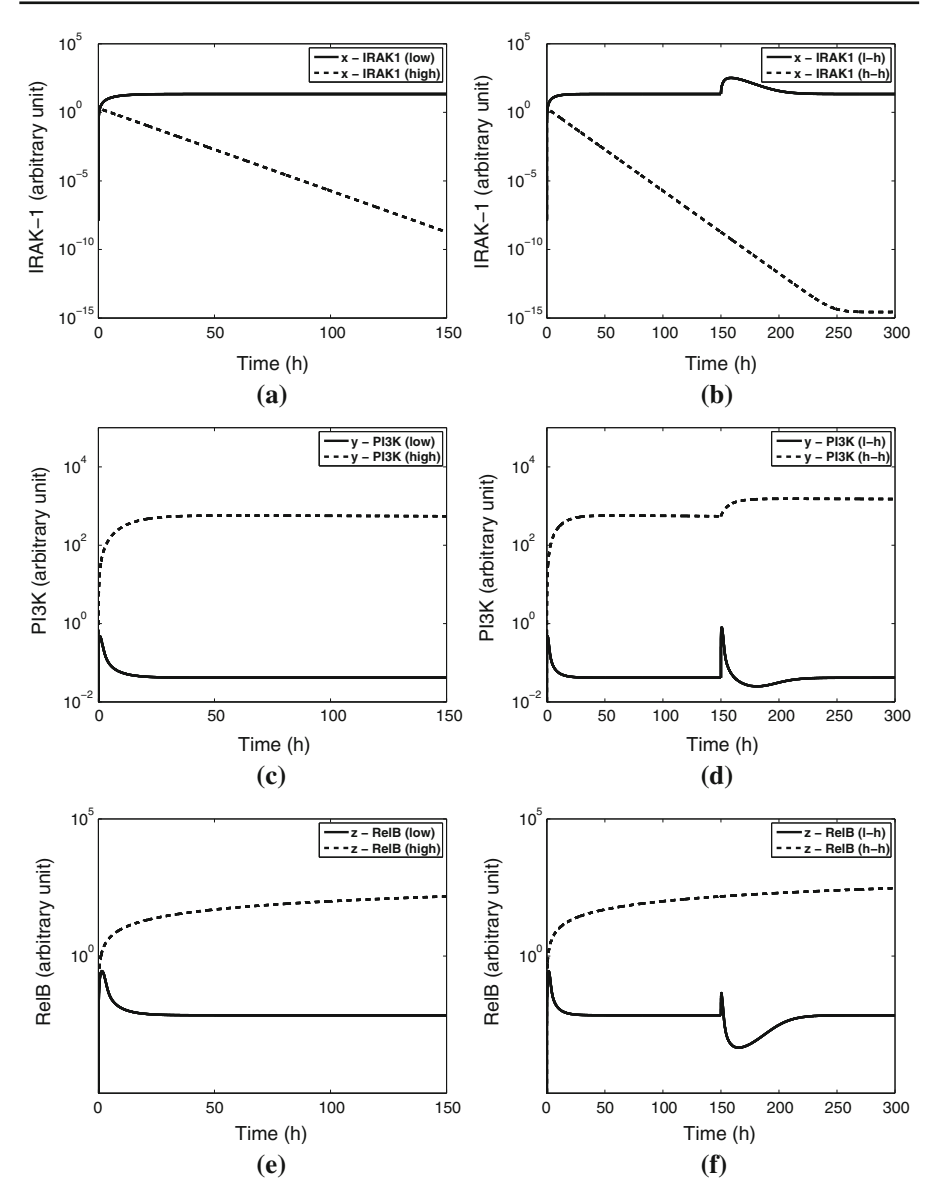


Fig. 3 Simulated dynamics of model (1) for: (left) single challenge with high ( $L_0=100$ , dashed lines) and a super-low ( $L_0=0.1$ , solid lines) LPS; (right) two sequential LPS challenges with second challenge applied 150h after primary challenge, and either high-high doses (dashed lines) or super low- high doses (solid lines). All parameters as in Table 1. a IRAK-1 dynamics following primary challenge. b IRAK-1 dynamics following primary and secondary challenge. c PI3K dynamics following primary and secondary challenge. e RelB dynamics following primary and secondary challenge.



three proteins follows the outcomes seen after super-low primary LPS dose. Indeed, the high booster does not change the equilibria of IRAK-1, PI3K or RelB (Fig. 3b, solid curves). In particular, RelB decreases transiently before increasing to the before the booster low equilibrium. Therefore, both primary and secondary responses are representative of a strong inflammatory response (primed state). These results show, that under these initial conditions, the macrophage phenotype is determined during the primary stimuli. We will next show how these results can be altered if the booster stimulus is super high.

#### 3.3 Secondary Challenge with a Phenotype Switch

The model predicts distinct dynamics of the three proteins for high-high LPS challenge compared to super low-high LPS challenges, with the size of the first dose determining the outcome during the secondary challenge, i.e., inflammation for primary super-low LPS and tolerance for primary high LPS. This result is dependent on the size of the booster. Indeed, the bistable nature of the system predicts a possible switch in macrophage phenotype, depending on the chosen initial conditions. In particular, we found that we can drive the system in a different state by increasing the dose size. For a super-high primary LPS challenge,  $L_0 = 250$ , the RelB will have a high equilibrium (tolerant state,  $E_1$ ) no matter how high the booster size. On the other hand, a super-high LPS boosting,  $L_0 = 250$ , following a super-low primary LPS challenge can induce a phenotype switch, driving the system from the pro-inflammatory equilibrium  $(E_2)$  to the pro-tolerant equilibrium  $(E_1)$  (Fig. 4). Indeed, the super low–super high challenges will drive RelB from low-to-high levels (see Fig. 4f, solid line), corresponding to macrophage phenotype changes from pro-inflammatory to pro-tolerant. The increase in PI3K caused by the super-high secondary dose counteracts the IRAK-1 increase (see Fig. 4b, d, solid line), resulting in decreased inhibition of PI3K and an increase in RelB levels. By contrast, high-dose boosting of  $L_0 = 100$  yields the inhibition of PI3K by IRAK-1 as the factor determining the system's dynamics by not allowing for high enough PI3K levels which would inhibit the IRAK-1 production (see Fig. 3b, d, solid line). Therefore, the systems stay in a pro-tolerant state.

Besides its strength, the timing of the secondary LPS challenge plays a role in the outcome as well. An early high ( $L_0=100$ ) booster t=5 h after primary super-low challenge, drives the system from primed to tolerant. A later high ( $L_0=100$ ) booster t=10, (75, 150) hours after primary super-low challenge, only leads to transient changes and does not drive the system into another immune state (see Fig. 5). In experiments, the cells are usually primed overnight, *i.e.*, for at least 6 h (Maitra et al. 2011; Henricson et al. 1990). Our model predicts that, if the primary challenge was super low, boosting with high-dose ( $L_0=100$ ) in a shorter than 6 h span following primary challenge, will drive the system into a tolerant state with elevated RelB. By contrast, if the primary challenge was super low, boosting at times later than a 6 h span following primary challenge, will keep the system in a pro-inflammatory state with low RelB levels. A bifurcation diagram for the asymptotic dynamics of RelB versus both the booster timing and size when the primary LPS challenge is weak ( $L_0=0.1$ ) is shown in Fig. 6.



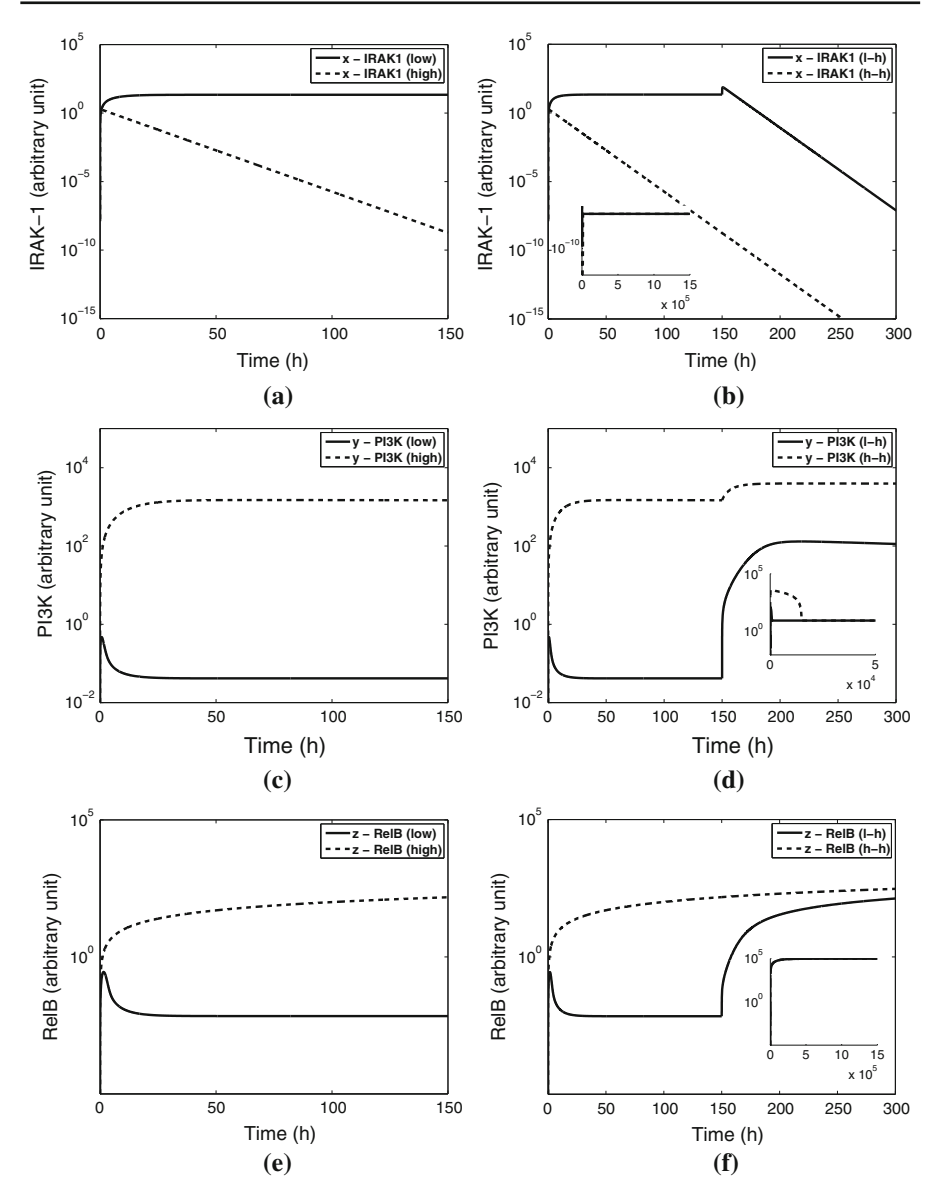


Fig. 4 Simulated dynamics of model (1) for: (left) single challenge with high ( $L_0=250$ , dashed lines) and a super-low ( $L_0=0.1$ , solid lines) LPS; (right) two sequential LPS challenges with second challenge applied 150h after primary challenge, and either high-high doses (dashed lines) or super low-high doses (solid lines), including the asymptotic behavior. All parameters as in Table 1. a IRAK-1 dynamics following primary challenge. b IRAK-1 dynamics following primary and secondary challenge. c PI3K dynamics following primary challenge. d PI3K dynamics following primary and secondary challenge. e RelB dynamics following primary and secondary challenge.



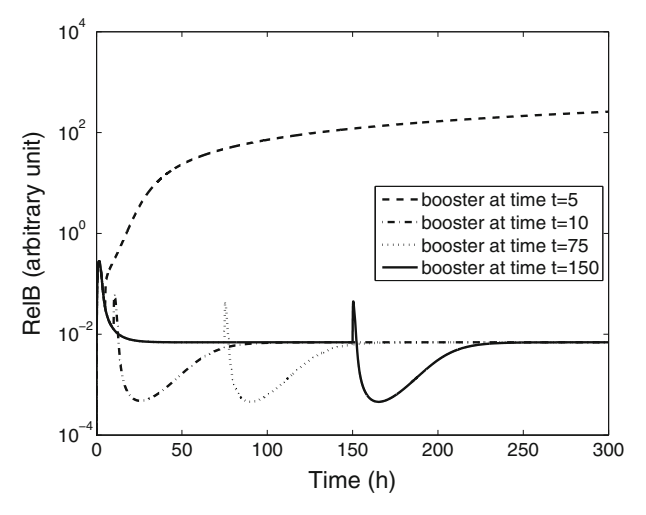


Fig. 5 RelB dynamics for super-low ( $L_0 = 0.1$ ) followed by high ( $L_0 = 100$ ) LPS challenges, when the challenge is applied at different times. All parameters as in Table 1

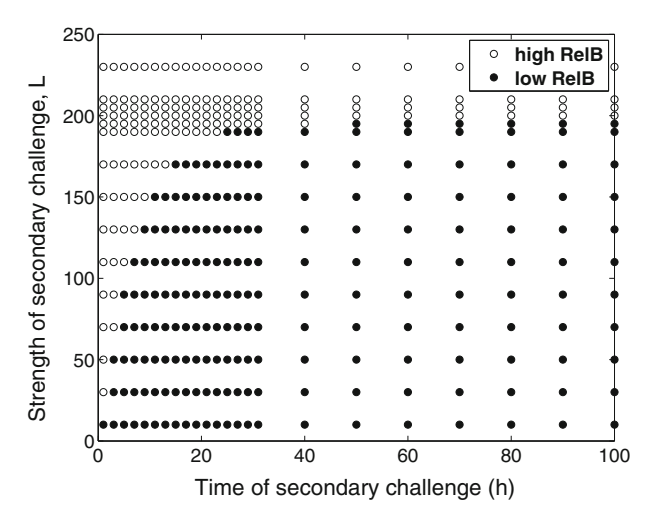


Fig. 6 Boosting after a super-low ( $L_0=0.1$ ) primary challenge. Dependence of the RelB equilibria on the time and strength of the booster. All parameters as in Table 1

#### 4 Discussion

We developed a mathematical model describing the differential response in macrophages function between pro-inflammatory and pro-tolerant phenotypes when challenged with LPS. Previous modeling studies have investigated cellular programming into different phenotypes by either describing the topology of the transcription-factor networks underlying such switch through the use of generic deterministic models describing the topological motifs of bistability (Fu et al. 2012; Tyson et al. 2001, 2003; Tyson and Novak 2010) and inflammation (Reynolds et al. 2006; Day et al. 2006),



by characterizing the global architecture of cell phenotype (Wang et al. 2014; Bhattacharya et al. 2011), and by describing the biochemical network models involved in cell fate (Ramsey et al. 2005; Bornholdt 2005). Such models could be applied to describe the switch in the macrophage phenotype, but would not predict the mechanisms behind the switch. In this study, we model the biochemical kinetics of three molecules involved in macrophage priming: IRAK-1, PI3K, and RelB. By investigating their dynamics, we connected the immunological outcomes with the size of bacterial endotoxin challenge.

Our model exhibits bistable behavior, with the motif of bistability being induced by the nonlinear mutual inhibition of proteins IRAK-1 and PI3K. We found that the pro-tolerant and pro-inflammatory macrophage states are determined by the size of the initial LPS dose, with a super-low primary LPS leading to inflammation and high primary LPS leading to tolerance. Perturbing these initial states is highly dependent on the size of LPS boosting and is one directional. Once we have a tolerant macrophage response (following a high LPS primary challenge), we cannot revert to an inflammatory macrophage response no matter the size of the LPS booster. If the system is in an inflammatory state (following a super-low LPS primary challenge), however, a high and early LPS booster can revert the macrophages into pro-tolerant cells. These results are based on the connection between RelB levels and the phenotypes of the macrophages.

One model limitation is the assumption that the decay of PI3K needs to be modeled in a density-dependent manner. When we change this to the more classical linear-type decay, we maintain bistable kinetics, but we lose the RelB qualitative behavior, *i.e.*, the observed low RelB level for low initial LPS stimuli and high RelB level for high initial LPS stimuli.

Under the model parameters, we quantified the timing and size of LPS booster needed to observe this switch in phenotype. These results may be useful to study mechanisms of autoimmune diseases. Autoimmunity refers to diseases in which the body's own immune system will attack healthy cells, typically through inflammation. In reducing the body's immune response, and thus inflammation, damage to host tissue can be minimized (Navegantes et al. 2017).

Our model was able to qualitatively match the IRAK-1, PI3K, and RelB dynamics and half-lives observed experimentally following a single endotoxin challenge with an increase in IRAK-1 and decay of PI3K and RelB following super-low-dose LPS challenge; decreased IRAK-1 and increased PI3K and RelB following high-dose LPS challenge (Deng et al. 2013). We could not, however, determine their physiological levels as many of the model parameters are unitless. Quantitative knowledge of such parameters is needed to quantitatively match the three proteins concentrations with the decision-making predictions given by our model.

In conclusion, we determined a molecular model that can explain the differential responses between macrophage phenotypes and connected the outcomes with the size of LPS primary doses. Our results can be used to guide treatments for patients with either autoimmune diseases or a compromised immune system.

**Acknowledgements** Funding was provided by Simons Foundation (Grant No. 427115) and National Science Foundation (Grant No. 1813011).



#### **Appendix**

Here, we investigate the positivity and boundness of the following system's solutions [system (1)].

$$\frac{\mathrm{d}x}{\mathrm{d}t} = \frac{c_x + a_x L}{b_x^m + y^m} - d_x x,$$

$$\frac{\mathrm{d}y}{\mathrm{d}t} = \frac{c_y + a_y L}{b_y + x} - d_y \frac{y}{b_v + y},$$

$$\frac{\mathrm{d}z}{\mathrm{d}t} = \frac{a_z y}{b_z + y} - d_z z \frac{x}{b_z + y},$$

$$\frac{\mathrm{d}L}{\mathrm{d}t} = -d_L L.$$
(11)

Assume that  $b_x^m = b_y = b_z = b_v = 1$  and all other parameters parm =  $\{a_x, d_x, c_y, a_y, d_y, a_z, d_z, d_L, m\}$  are positive. Let  $w(t) := [x(t), y(t), z(t), L(t)]^T$  be the solution vector and  $u(t) := [x(t), y(t), z(t)]^T$  be the vector that considers the first three variables. Consider the following functions

$$g(t, w) = \begin{pmatrix} g_1 \\ g_2 \\ g_3 \\ g_4 \end{pmatrix} = \begin{pmatrix} \frac{c_x + a_x L}{b_x^w + y^m} - d_x x, \\ \frac{c_y + a_y L}{b_y + x} - d_y \frac{y}{b_v + y} \\ \frac{a_z y}{b_z + y} - d_z z \frac{x}{b_z + y} \\ -d_L L \end{pmatrix},$$

$$f: \mathbb{R}_+^3 \to \mathbb{R}^3 \text{ given by}$$

$$f(t, u) = \begin{pmatrix} g_1 \\ g_2 \\ g_3 \end{pmatrix},$$

$$(12)$$

and the following initial value problem

$$w'(t) = g(t, w),$$
  
subject to (13)  
 $x(0) = x_0 > 0, \ y(0) = y_0 > 0, \ z(0) = z_0 > 0, \ L(0) = L_0 > 0.$ 

We want to show that the solutions of the initial value problem (13) are positive and bounded. The fourth variable L(t) yields

$$L(t) = L_0 e^{-d_L t} \in (0, L_0], \text{ for all } t \in [0, \infty).$$
 (14)

The initial value problem (13) reduces to

$$u'(t) = f(t, u),$$
  
subject to (15)  
 $x(0) = x_0 > 0, \ y(0) = y_0 > 0, \ z(0) = z_0 > 0,$ 



where  $L(t) = L_0 e^{-d_L t}$ .

**Proposition 1** *There exists a positive number*  $\beta > 0$  *such that system* (13) *has a unique positive solution on*  $[0, \beta)$ .

**Proof** Since f is continuously differentiable on  $\mathbb{R}^3_+$ , it is locally Lipschitz on  $\mathbb{R}^3_3$ . By Thm. 2, there exists a maximal value  $\beta > 0$  such that (15) has a unique solution on the interval  $[0, \beta)$  with values in  $\mathbb{R}^3_+$ .

**Proposition 2** The solution of (15) exists and is positive in  $\mathbb{R}^3_+$ . Furthermore, if  $c_y < d_y$  the solution is bounded.

**Proof** Assume that  $\beta$  found in Proposition 1 is finite. Since x(t), y(t), z(t), L(t) > 0 and L is decreasing on  $[0, \beta)$ , the following inequalities hold for all  $t \in [0, \beta)$ 

$$\frac{dx}{dt} = \frac{c_x + a_x L}{1 + y^m} - d_x x < c_x + a_x L_0, 
\frac{dy}{dt} = \frac{c_y + a_y L}{1 + x} - d_y \frac{y}{1 + y} < c_y + a_y L_0, 
\frac{dz}{dt} = a_z \frac{y}{1 + y} - d_z \frac{xz}{1 + y} < a_z.$$
(16)

This yields

$$x(t) < x_0 + (c_x + a_x L_0)t < x_0 + (c_x + a_x L_0)\beta := x_{\text{max}},$$
  

$$y(t) < y_0 + (c_y + a_y L_0)t < y_0 + (c_y + a_y L_0)\beta := y_{\text{max}},$$
  

$$z(t) < z_0 + a_z t < z_0 + a_z \beta := z_{\text{max}}.$$
(17)

for all  $t \in [0, \beta)$ . Thus, x, y and z are bounded from above on  $[0, \beta)$ . Using

$$\frac{dx}{dt} = \frac{c_x + a_x L}{1 + y^m} - d_x x \ge \frac{c_x}{1 + y_{\text{max}}^m} - d_x x, 
\frac{dy}{dt} = \frac{c_y + a_y L}{1 + x} - d_y \frac{y}{1 + y} \ge \frac{c_y}{1 + x_{\text{max}}} - d_y y, \tag{18}$$

we find that if  $x \le \frac{c_x}{d_x(1+y_{\max}^m)}$ , then  $\frac{dx}{dt} \ge 0$ . Similarly, if  $y \le \frac{c_y}{d_y(1+x_{\max})}$  then  $\frac{dy}{dt} \ge 0$ . Therefore

$$x(t) \ge \min\left\{x_0, \frac{c_x}{d_x(1+y_{\max}^m)}\right\} := x_{\min} > 0, \text{ for all } t \in [0, \beta),$$
 (19)

and

$$y(t) \ge \min \left\{ y_0, \frac{c_y}{d_y(1 + x_{\text{max}})} \right\} := y_{\text{min}} > 0, \text{ for all } t \in [0, \beta).$$
 (20)

Lastly, since

$$\frac{dz}{dt} = \frac{a_z y}{1 + v} - d_z \frac{xz}{1 + v} \ge \frac{a_z y_{\min}}{1 + v_{\max}} - d_z \frac{x_{\max}}{1 + v_{\min}} z,$$
(21)



for all  $t \in [0, \beta)$ , we have that if  $z \leq (\frac{a_z y_{\min}}{1 + y_{\max}})/(d_z \frac{x_{\max}}{1 + y_{\min}})$  then  $\frac{dz}{dt} \geq 0$ . Thus

$$z(t) \ge \min\left\{z_0, \left(\frac{a_z y_{\min}}{1 + y_{\max}}\right) / \left(d_z \frac{x_{\max}}{1 + y_{\min}}\right)\right\} := z_{\min} > 0, \quad \text{for all } t \in [0, \beta).$$
(22)

Therefore, x, y and z are bounded from below on  $[0, \beta)$ . If  $\beta$  is finite, there are positive lower and upper bounds for x, y and z on  $[0, \beta)$ , i.e.,  $u = [x, y, z]^T$  is bounded on  $[0, \beta)$ . Since f is continuous, f(u) is bounded on  $[0, \beta)$ . By 3° of Thm.  $2 \lim_{t \to \beta} x(t) = 0$ , or  $\lim_{t \to \beta} y(t) = 0$ , or  $\lim_{t \to \beta} z(t) = 0$ . This contradicts the positive lower bounds of x, y and z. Thus  $\beta = \infty$ .

It remains to show that for  $c_y < d_y$ , the solutions are bounded on  $[0, \infty)$ . We know that x, y, z > 0 for  $t \in [0, \infty)$ . We have

$$\frac{dx}{dt} = \frac{c_x + a_x L}{1 + v^m} - d_x x \le c_x + a_x L_0 - d_x x, \text{ for all } t \ge 0,$$
(23)

which yields that if  $x \ge \frac{c_x + a_x L_0}{d_x}$  then  $\frac{dx}{dt} \le 0$ . Hence

$$x(t) \le \max \left\{ x_0, \frac{c_x + a_x L_0}{d_x} \right\} =: x_{\max}^1, \text{ for all } t > 0.$$
 (24)

Since  $\lim_{t\to\infty} L(t) = 0$  and  $c_y < d_y$ , there exists a constant  $t_1 > 0$  such that

$$c_{\mathcal{V}} + a_{\mathcal{V}} L(t) < d_{\mathcal{V}}, \tag{25}$$

and

$$L(t) \le L(t_1) =: L_1,$$
 (26)

for  $t > t_1$ . Then

$$\frac{dy}{dt} = \frac{c_y + a_y L}{1 + x} - d_y \frac{y}{1 + y} \le c_y + a_y L_1 - d_y \frac{y}{1 + y}, \quad \text{for all } t \ge t_1.$$
 (27)

Therefore, using  $c_y + a_y L_1 < d_y$  we obtain that for  $t \in [t_1, \infty)$ , if  $y \ge \frac{c_y + a_y L_1}{d_y - c_y - a_y L_1}$ , then  $\frac{dy}{dt} \le 0$ . Furthermore, y is continuous, therefore bounded on the closed interval  $[0, t_1]$ . Thus, for  $t \in [0, \infty)$ 

$$y(t) \le \max \left\{ \max_{t \in [0, t_1]} y(t), \frac{c_y + a_y L_1}{d_y - c_y - a_y L_1} \right\} =: y_{\text{max}}^1.$$
 (28)

As in Eq. (19)

$$x(t) \ge \min \left\{ x_0, \frac{c_x}{d_x \left( 1 + y_{\text{max}}^{1 m} \right)} \right\} =: x_{\text{min}}^1 > 0, \text{ for all } t > 0.$$
 (29)



As in Eq. (20), we have

$$y(t) \ge \min \left\{ y_0, \frac{c_y}{d_y \left( 1 + x_{\text{max}}^1 \right)} \right\} =: y_{\text{min}}^1 > 0, \text{ for all } t > 0.$$
 (30)

To find an upper bound of z we use

$$\frac{dz}{dt} = \frac{a_z y}{1 + y} - d_z \frac{z x}{1 + y} \le a_z - d_z \frac{x_{\min}^1}{1 + y_{\max}^1} z.$$
 (31)

This yields

$$z(t) \le \max \left\{ z_0, \frac{a_z}{d_z \frac{x_{\min}^1}{1 + y_{\max}^1}} \right\} =: z_{\max}^1, \quad t \ge 0.$$
 (32)

Lastly, to find a lower bound for z(t) we use

$$z(t) \ge \min \left\{ z_0, \left( \frac{a_z y_{\min}^1}{1 + y_{\max}^1} \right) / \left( d_z \frac{x_{\max}^1}{1 + y_{\min}^1} \right) \right\} =: z_{\min}^1 > 0, \quad \text{for all } t \ge 0. \quad (33)$$

Thus, we have shown that there is a unique solution of (13) on  $[0, \infty)$  that is positive and bounded.

**Proposition 3** An equilibrium solution of system (1) with  $b_x = b_y = b_z = 1$  is locally asymptotically stable if and only if  $\frac{AB}{m} > \bar{y}^{m+1}\bar{x}^2$ , where  $A = \frac{c_y}{d_y}$  and  $B = \frac{c_x}{d_x}$ .

**Proof** Let  $(\bar{x}, \bar{y}, \bar{z}, \bar{L})$  be an equilibrium solution of system (1). From (14) it follows that  $\lim_{t\to\infty} L(t) = 0$ , therefore we set  $\bar{L} = 0$ . Further, it follows from the proof of Proposition 2 that  $\bar{x}, \bar{y}, \bar{z} > 0$ . The Jacobian of system (1) evaluated at  $(\bar{x}, \bar{y}, \bar{z}, \bar{L})$  is given by

$$J = \begin{pmatrix} -d_{x} & -\frac{c_{x}m\bar{y}^{m+1}}{(1+\bar{y}^{m})^{2}} & 0 & -\frac{a_{x}}{1+\bar{y}^{m}} \\ -\frac{c_{y}}{(1+\bar{x})^{2}} & -\frac{d_{y}}{(1+\bar{y})^{2}} & 0 & \frac{a_{y}}{1+\bar{x}} \\ -\frac{d_{z}\bar{z}}{1+\bar{y}} & \frac{a_{z}}{(1+\bar{y})^{2}} + \frac{d_{z}\bar{z}\bar{x}}{(1+\bar{y})^{2}} & -\frac{d_{z}\bar{x}}{1+\bar{y}} & 0 \\ 0 & 0 & 0 & -d_{L} \end{pmatrix}.$$
(34)

Two eigenvalues of J are given by  $\lambda_1 = -d_L < 0$  and  $\lambda_2 = -\frac{d_z\bar{x}}{1+\bar{y}} < 0$ . The remaining two eigenvalues  $\lambda_3$  and  $\lambda_4$  satisfy the equation

$$(\lambda + a)(\lambda + d) - cb = 0, (35)$$

where  $a = d_x$ ,  $b = \frac{c_x m \bar{y}^{m-1}}{(1 + \bar{y}^m)^2}$ ,  $c = \frac{c_y}{(1 + \bar{x})^2}$ , and  $d = \frac{d_y}{(1 + \bar{y})^2}$ . Since a, b, c, d > 0 this implies that

$$\lambda_{3,4} = -\frac{a+d}{2} \pm \sqrt{\frac{(a+d)^2}{4} - (ad-bc)}$$
 (36)



have negative real parts iff ad > bc, which is equivalent to

$$\frac{d_{x}d_{y}}{(1+\bar{y})^{2}} > \frac{c_{x}c_{y}m\bar{y}^{m-1}}{(1+\bar{y}^{m})^{2}(1+\bar{x})^{2}}$$

$$\iff \frac{d_{x}d_{y}}{(1+\bar{y})^{2}} > c_{y}c_{x}m\bar{y}^{m-1}\left(\frac{1}{1+\bar{y}^{m}}\right)^{2}\left(\frac{1}{1+\bar{x}}\right)^{2}$$

$$\iff \frac{d_{x}d_{y}}{(1+\bar{y})^{2}} > c_{y}c_{x}m\bar{y}^{m-1}\left(\frac{d_{x}}{c_{x}\bar{x}}\right)^{2}\left(\frac{d_{y}}{c_{y}}\frac{\bar{y}}{1+\bar{y}}\right)^{2}$$

$$\iff \frac{c_{x}c_{y}}{d_{x}d_{y}m} > \bar{y}^{m+1}\bar{x}^{2}$$

$$\iff \frac{AB}{m} > \bar{y}^{m+1}\bar{x}^{2}.$$
(37)

We have shown that all eigenvalues of J have negative real part, hence an equilibrium is locally asymptotically stable, iff  $\frac{AB}{m} > \bar{y}^{m+1}\bar{x}^2$ . 

**Proposition 4** If  $0 < m \le 1$  then system (1) has at most two positive equilibria.

**Proof** We find that if  $E = (\bar{x}, \bar{y}, \bar{z}, \bar{L})$  is an equilibrium of system (1), then it satisfies

$$\bar{L} = 0,$$

$$\bar{x} = \frac{B}{1 + \bar{y}^m},$$

$$\bar{z} = \frac{a_z}{d_z} \cdot \frac{\bar{y}}{\bar{x}},$$
(38)

where  $\bar{y}$  satisfies the equation

$$\frac{B}{1 + \bar{y}^m} - \frac{A(1 + \bar{y}) - \bar{y}}{\bar{y}} = 0,$$

and  $A = \frac{c_y}{d_x}$  and  $B = \frac{c_x}{d_x}$ . Therefore system (1) has as many positive equilibria as

there are roots of the function  $g(y) = \frac{B}{1+\bar{y}^m} - \frac{A(1+\bar{y})-\bar{y}}{\bar{y}}$  in  $(0,\infty)$ . We find  $g(y) = \frac{By-[A(1+y)-y](1+y^m)}{(1+y^m)y}$ . Hence, g(y) = 0 if and only if f(y) = 0, where  $f(y) = By - [A(1+y)-y](1+y^m)$  is the numerator of g(y). Expanding f(y) and taking terms with the same powers of y together yields

$$f(y) = y^{m+1}(1-A) - Ay^m + (B-A+1)y - A.$$

Note that  $A = \frac{c_y}{d_y} < 1$  because  $c_y < d_y$ . f is a smooth function on  $(0, \infty)$ . Hence, for f to have at least three roots in  $(0, \infty)$  its second derivative needs to have a root in  $(0, \infty)$ . Using



$$f''(y) = (1 - A)(m + 1)my^{m-1} - Am(m - 1)y^{m-1}$$
$$= y^{m-2}[(1 - A)(m + 1)my - Am(m - 1)] = 0$$
$$\iff y = \frac{Am(m - 1)}{(1 - A)(m + 1)m}$$

Since  $A \in (0, 1)$ , the equation f''(y) = 0 has one solution in  $(0, \infty)$  if m > 1 and no solution in that interval otherwise. Therefore, f and hence g can have at most three solutions in  $(0, \infty)$  if m > 1 and at most two solution in  $(0, \infty)$  if  $m \le 1$ .

#### **Proposition 5** If m > 1 then system (1) has

- 1. either exactly one locally asymptotically stable equilibrium or
- 2. exactly two locally asymptotically stable and one unstable equilibrium or
- 3. exactly one locally asymptotically stable equilibrium and one equilibrium that is not locally asymptotically stable.

**Proof** Let g be defined as in proposition 4. In the proof of proposition 4, we have shown that g has at most three roots in  $(0, \infty)$ . Since g is a smooth function on  $(0, \infty)$ ,  $\lim_{y\to 0^+} g(y) = -\infty$  and  $\lim_{y\to \infty} g(y) = \infty$ , we find that g has

- 1. either one root  $y_1 \in (0, \infty)$  with  $g'(y_1) > 0$  and no other roots in  $(0, \infty)$  or
- 2. three distinct roots  $y_1, y_2, y_3 \in (0, \infty)$  with  $y_1 < y_2 < y_3$  and  $g'(y_1), g'(y_3) > 0$  and  $g'(y_2) < 0$  and no other roots in  $(0, \infty)$  or
- 3. one root  $y_1 \in (0, \infty)$  with  $g'(y_1) > 0$  and one root  $y_2 \in (0, \infty)$  with  $g'(y_2) = 0$  and no other roots in  $(0, \infty)$ .

We find

$$g'(y) = \frac{-Bmy^{m+1} + A(1+y^m)^2}{[(1+y^m)y]^2},$$

and therefore g'(y) > 0 if and only if

$$A(1+y^m)^2 > Bmy^{m+1}. (39)$$

for y in  $(0, \infty)$ . Let  $\bar{y}$  be a root of g. Then,  $\bar{y}$  is the y-value of an equilibrium of system (1) and the corresponding x-value is given by  $\bar{x} = \frac{B}{1+\bar{y}^m}$ . Using this in (39) we obtain

$$\frac{AB}{m} > \bar{y}^{m+1}\bar{x}^2,\tag{40}$$

which implies stability of the equilibrium corresponding to the root  $\bar{y}$  of g. Similarly, we can show that if  $\bar{y}$  is a root of g with  $g'(\bar{y}) < 0$ , then the equilibrium defined by  $\bar{y}$  is unstable. This implies that statements (1)–(3) are equivalent to the three statements in the formulation of the proposition.

#### References

Abd-Ellah A, Voogdt C, Krappmann D, Möller P, Marienfeld R (2018) GSK3 $\beta$  modulates NF- $\kappa$ b activation and relb degradation through site-specific phosphorylation of BCL10. Sci Rep 8(1):1352



- Arango Duque G, Descoteaux A (2014) Macrophage cytokines: involvement in immunity and infectious diseases. Front Immunol 5:491
- Bhattacharya S, Zhang Q, Andersen M (2011) A deterministic map of Waddington's epigenetic landscape for cell fate specification. BMC Syst Biol 5(1):85
- Biswas S, Lopez-Collazo E (2009) Endotoxin tolerance: new mechanisms, molecules and clinical significance. Trends Immunol 30(10):475–487
- Bornholdt S (2005) Less is more in modeling large genetic networks. Science 310(5747):449-451
- Chaurasia B, Mauer J, Koch L, Goldau J, Koch A, Brüning J (2010) Phosphoinositide-dependent kinase 1 provides negative feedback inhibition to toll-like receptor-mediated NF-κB activation in macrophages. Mol Cell Biol 30(17):4354–4366
- Chen X, El Gazzar M, Yoza BK, McCall CE (2009) The NF-κB factor RelB and histone H3 lysine methyltransferase G9a directly interact to generate epigenetic silencing in endotoxin tolerance. J Biol Chem 284(41):27857–27865
- Day J, Rubin J, Vodovotz Y, Chow CC, Reynolds A, Clermont G (2006) A reduced mathematical model of the acute inflammatory response II. Capturing scenarios of repeated endotoxin administration. J Theor Biol 242(1):237–256
- Deng H, Maitra U, Morris M, Li L (2013) Molecular mechanism responsible for the priming of macrophage activation. J Biol Chem 288(6):3897–3906
- Dillingh M, van Poelgeest E, Malone K, Kemper E, Stroes E, Moerland M, Burggraaf J (2014) Characterization of inflammation and immune cell modulation induced by low-dose LPS administration to healthy volunteers. J Inflamm (Lond) 11(1):28
- Fan H, Cook J (2004) Molecular mechanisms of endotoxin tolerance. J Endotoxin Res 10(2):71-84
- Fu Y, Glaros T, Zhu M, Wang P, Wu Z, Tyson J, Li L, Xing J (2012) Network topologies and dynamics leading to endotoxin tolerance and priming in innate immune cells. PLoS Comput Biol 8(5):e1002,526
- Goldbeter A (1995) A model for circadian oscillations in the drosophila period protein (per). Proc R Soc Lond B 261(1362):319–324
- Guha M, Mackman N (2001) LPS induction of gene expression in human monocytes. Cell Signal 13(2):85–94
- Henricson B, Benjamin W, Vogel S (1990) Differential cytokine induction by doses of lipopolysaccharide and monophosphoryl lipid A that result in equivalent early endotoxin tolerance. Infect Immun 58(8):2429–2437
- Hirohashi N, Morrison D (1996) Low-dose lipopolysaccharide (lps) pretreatment of mouse macrophages modulates LPS-dependent interleukin-6 production in vitro. Infect Immun 64(3):1011–1015
- Huang Y, Li T, Sane D, Li L (2004) IRAK1 serves as a novel regulator essential for lipopolysaccharideinduced interleukin-10 gene expression. J Biol Chem 279(49):51,697–51,703
- Hume D, Underhill D, Sweet M, Ozinsky A, Liew F, Aderem A (2001) Macrophages exposed continuously to lipopolysaccharide and other agonists that act via toll-like receptors exhibit a sustained and additive activation state. BMC Immunol 2(1):11
- Janeway CJ, Travers P, Walport M et al (2001) Immunobiology: the immune system in health and disease, 5th edn. Garland Science, New York
- Ko H, Kim C, Lee S, Song J, Lee K, Kim K, Park K, Cho S, Ahn J (2014) P42 Ebp1 regulates the proteasomal degradation of the p85 regulatory subunit of PI3k by recruiting a chaperone-E3 ligase complex HSP70/CHIP. Cell Death Dis 5(3):e1131
- Kollewe C, Mackensen A, Neumann D, Knop J, Cao P, Li S, Wesche H, Martin M (2004) Sequential autophosphorylation steps in the interleukin-1 receptor-associated kinase-1 regulate its availability as an adapter in interleukin-1 signaling. J Biol Chem 279(7):5227–5236
- Ma X, Yan W, Zheng H, et al. (2015) Regulation of IL-10 and IL-12 production and function in macrophages and dendritic cells. F1000Res. https://doi.org/10.12688/f1000research.7010.1
- Maitra U, Gan L, Chang S, Li L (2011) Low-dose endotoxin induces inflammation by selectively removing nuclear receptors and activating CCAAT/enhancer-binding protein δ. J Immunol 186(7):4467–4473
- Medvedev A, Kopydlowski K, Vogel S (2000) Inhibition of lipopolysaccharide-induced signal transduction in endotoxin-tolerized mouse macrophages: dysregulation of cytokine, chemokine, and toll-like receptor 2 and 4 gene expression. J Immunol 164(11):5564–5574
- Morris M, Li L (2012) Molecular mechanisms and pathological consequences of endotoxin tolerance and priming. Arch Immunol Ther Exp (Warsz) 60(1):13–18



Navegantes KC, Gomes RS, Pereira PAT, Czaikoski PG, Azevedo CHM, Monteiro MC (2017) Immune modulation of some autoimmune diseases: the critical role of macrophages and neutrophils in the innate and adaptive immunity. J Transl Med 15(1):36

- Noubir S, Hmama Z, Reiner N (2004) Dual receptors and distinct pathways mediate interleukin-1 receptorassociated kinase degradation in response to lipopolysaccharide. J Biol Chem 279:25,189–25,195
- Ramsey S, Orrell D, Bolouri H (2005) Dizzy: stochastic simulation of large-scale genetic regulatory networks. J Bioinform Comput Biol 3(02):415–436
- Reynolds A, Rubin J, Clermont G, Day J, Vodovotz Y, Ermentrout GB (2006) A reduced mathematical model of the acute inflammatory response: I. Derivation of model and analysis of anti-inflammation. J Theor Biol 242(1):220–236
- Shi C, Pamer EG (2011) Monocyte recruitment during infection and inflammation. Nat Rev Immunol 11(11):762–774
- Shnyra A, Brewington R, Alipio A, Amura C, Morrison D (1998) Reprogramming of lipopolysaccharideprimed macrophages is controlled by a counterbalanced production of IL-10 and IL-12. J Immunol 160(8):3729–3736
- Sun J, Ugolini S, Vivier E (2014) Immunological memory within the innate immune system. EMBO J 33(12):1295–1303
- Tyson J, Novak B (2010) Functional motifs in biochemical reaction networks. Annu Rev Phys Chem 61:219-240
- Tyson J, Chen K, Novak B (2001) Network dynamics and cell physiology. Nat Rev Mol Cell Biol 2:908–916 Tyson J, Chen K, Novak B (2003) Sniffers, buzzers toggles and blinkers: dynamics of regulatory and signaling pathways in the cell. Curr Opin Cell Biol 15:221–231
- Wang P, Song C, Zhang H, Wu Z, Tian XJ, Xing J (2014) Epigenetic state network approach for describing cell phenotypic transitions. Interface Focus 4(3):20130,068
- West M, Heagy W (2002) Endotoxin tolerance: a review. Crit Care Med 30(1):S64-S73
- West M, Koons A (2008) Endotoxin tolerance in sepsis: concentration-dependent augmentation or inhibition of LPS-stimulated macrophage TNF secretion by LPS pretreatment. J Trauma 65(4):893–900
- Wysocka M, Robertson S, Riemann H, Caamano J, Hunter C, Mackiewicz A, Montaner L, Trinchieri G, Karp C (2001) IL-12 suppression during experimental endotoxin tolerance: dendritic cell loss and macrophage hyporesponsiveness. J Immunol 166(12):7504–7513
- Yamin T, Miller D (1997) The interleukin-1 receptor-associated kinase is degraded by proteasomes following its phosphorylation. J Biol Chem 272:21,540–21,547
- Yuan R, Li L (2016) Dynamic modulation of innate immunity programming and memory. Sci China Life Sci 59(1):38–43
- Zhang J, An J (2007) Cytokines, inflammation and pain. Int Anesthesiol Clin 45(2):27–37
- Zhang X, Morrison D (1993) Lipopolysaccharide-induced selective priming effects on tumor necrosis factor alpha and nitric oxide production in mouse peritoneal macrophages. J Exp Med 177(2):511–516
- Ziegler-Heitbrock H (1995) Molecular mechanism in tolerance to lipopolysaccharide. J Inflamm 45(1):13–26

